Jet substructure performance and measurements in ATLAS

Mario Campanelli
University College London
On behalf of the ATLAS collaboration

EDS Blois Vietnam 2019

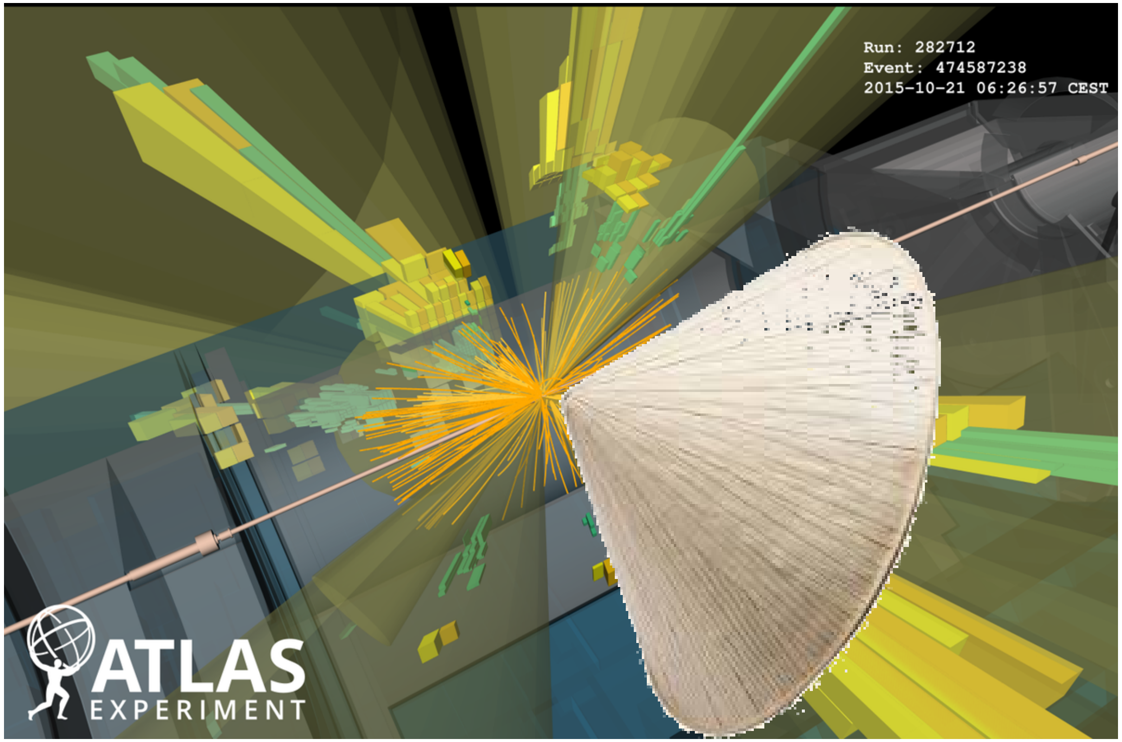

- Performance and phenomenology
  - Large-R jet calibration
  - Bottom-up uncertainties
  - Jet shapes
  - Top/W tagging
  - Soft-drop
- Measurements
  - SoftDrop jet mass
  - SoftDrop and Trimmed Jet shapes

Jets in ATLAS

- Internal structure of jets interesting to study QCD and to distinguish jets coming from light quarks, gluons or hadronic decays of heavy particles (W, Z,top, H…)
- Many different types of jets are used in ATLAS:
  - R = 0.2, 0.4, 0.6, 0.8, 1.0, variable-R
  - Calorimeter-based, p-flow (PF0 and TCC), track-assisted, ReClustered
- For substructure studies, so far most of results for calorimeter-based large-R jets

Initial constituents for calorimeter jets are topological clusters, supposed to represent a particle deposition
Starting from a cell 4σ above noise, neighbouring cells with 2σ and a surrounding layer are added.
Splitting algorithm separates nearby cluster, and a calibration is applied to account for non-compensation, dead material and out-of-cluster effects

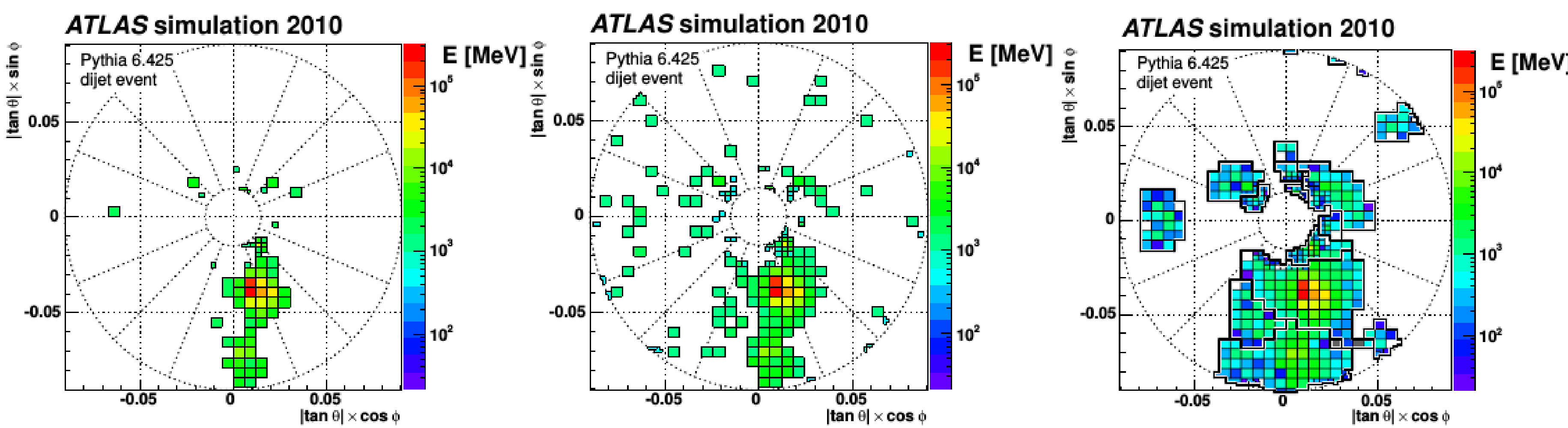

TopoClusters are then merged into jets using the anti-kt algorithm
→ cluster and jet calibrations and uncertainties are very important

Jet calibration

Jets are calibrated using a combination of MC- and data-based methods. Steps for small-R:

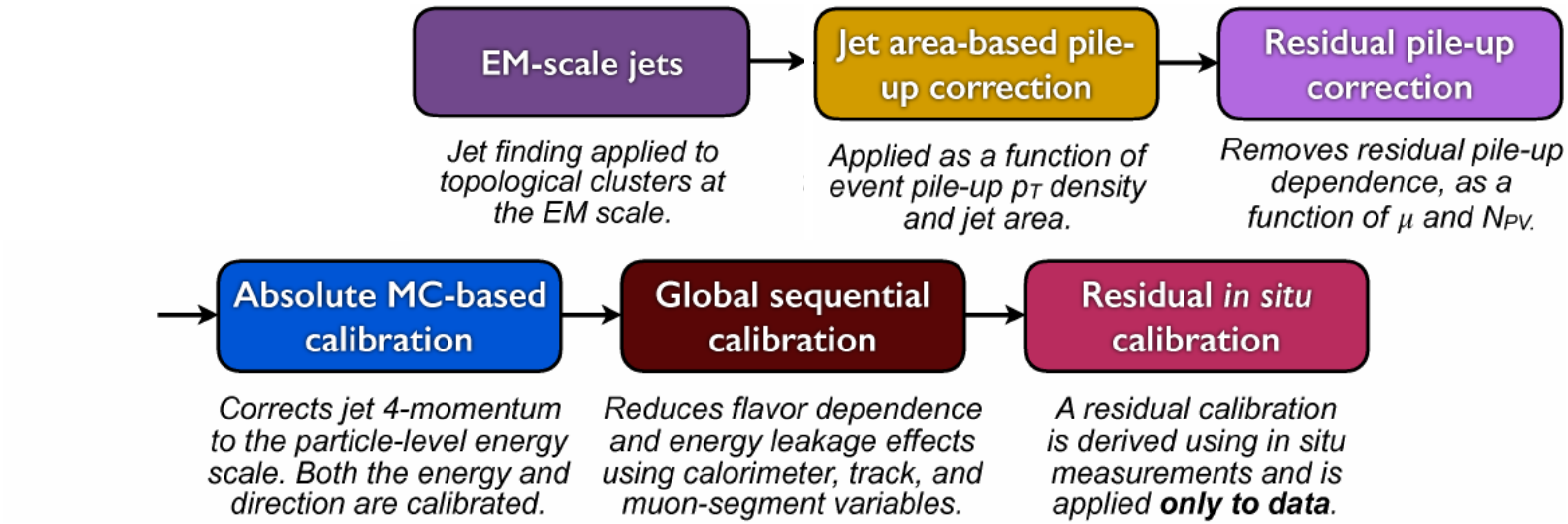

For large-R jets an additional grooming procedure (by default trimming, that removes k_T R = 0.2 subjets with <5% of jet p_T) can be applied before a dedicated MC and in-situ calibration

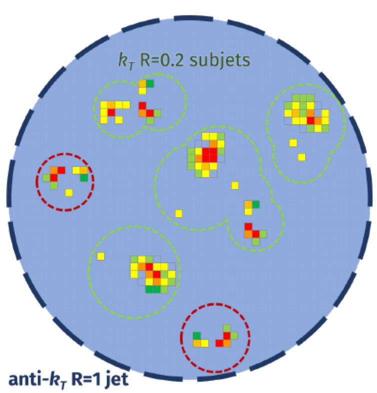

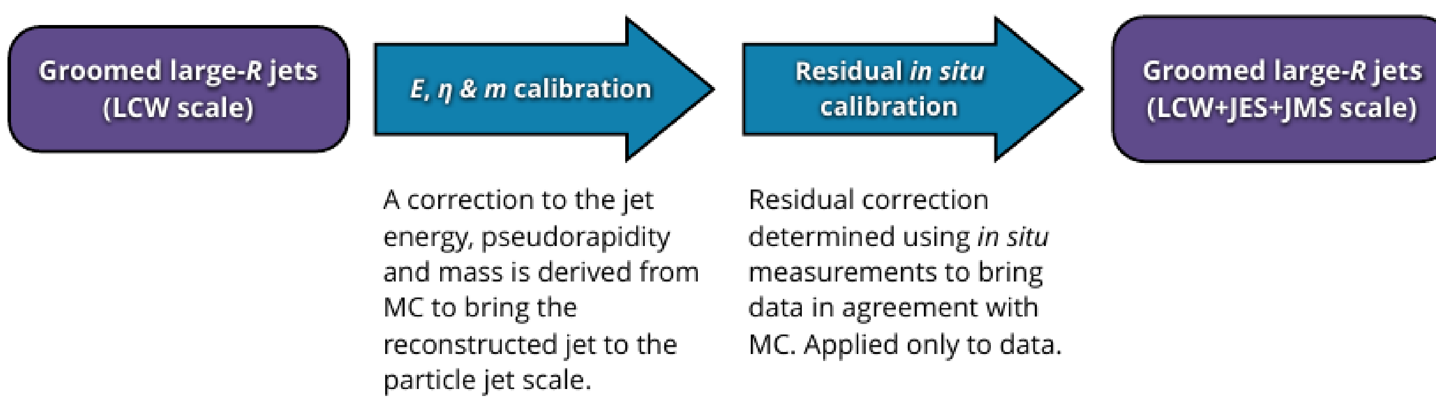

In-situ energy calibration

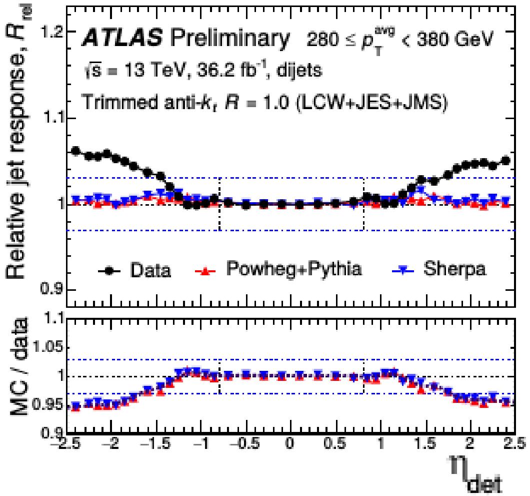

Even after jets are corrected to particle level, residual central-forward asymmetries in data are corrected to achieve a uniform response

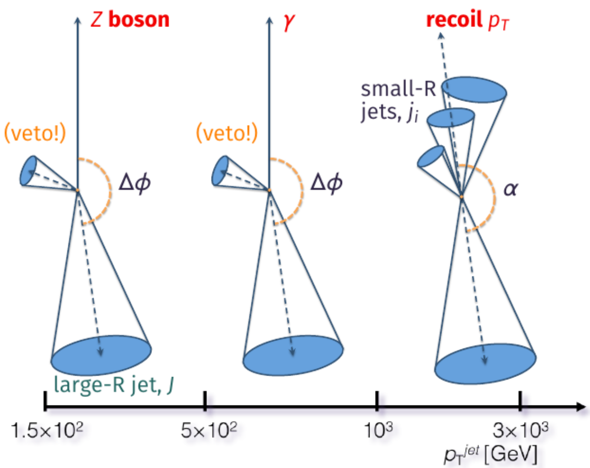

Jet energy further calibrated in-situ by balancing the response with well-measured objects (photons, Z→ll, small-R jets).

This "top-down" approach calibrates and provides uncertainties for average values, not differential quantities.

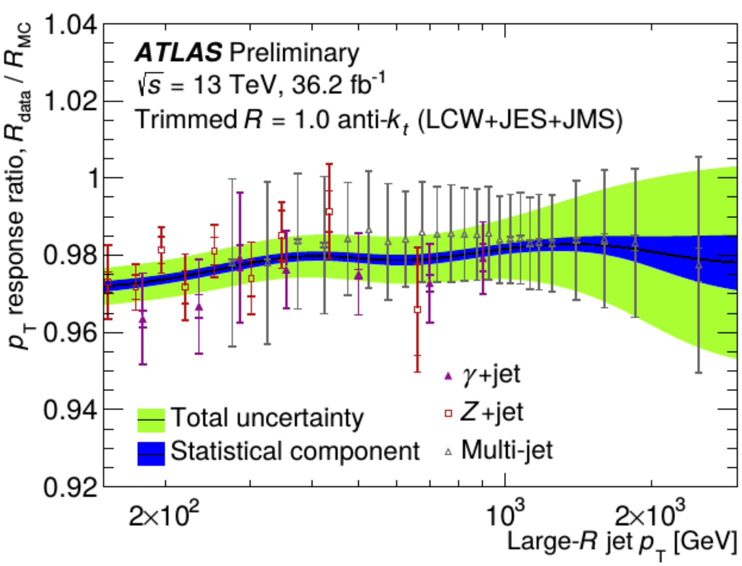

The results for the balancing methods are combined into a pt-dependent scale factor, used to rescale the whole jet 4-momentum.

Eur. Phys. J. C 79 (2019) 135

Bottom-up uncertainties from clusters

Calibrations and uncertainties on jets as 4-vectors are only the first step for a substructure measurement. Jet constituents are combined to produce more variables, like the jet mass, jet shapes etc.

Uncertainties on these quantities computed directly from the topoclusters, using a bottom-up approach

Cluster reconstruction efficiency, energy scale and resolution obtained from E/p on simulated isolated pion interactions

Uncertainties are applied to jet mass and shapes by smearing TopoCluster efficiency, energy and positions around these mean values

Additional uncertainties come from different assumptions on:
- energy correlations between clusters
- fractions of non-pion hadrons
- cluster splitting and merging

Bottom-up uncertainties have comparable size to top-down uncertainties computed from track/calo ratios, (only possible for average quantities not distributions)

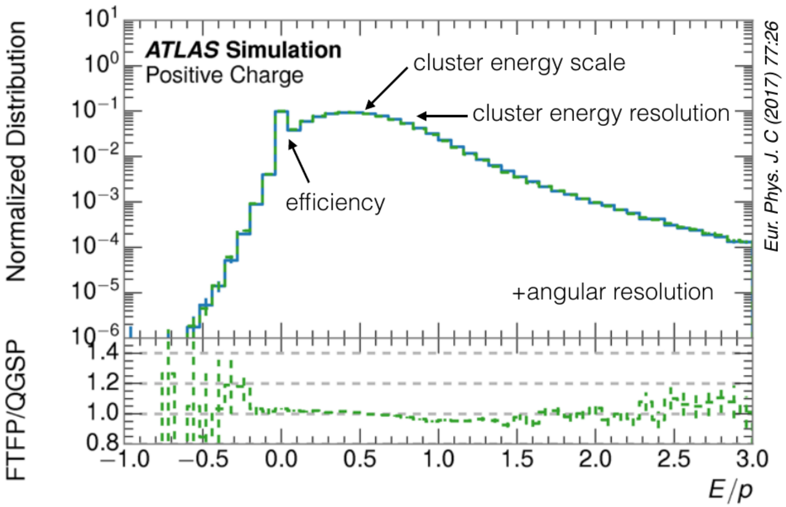

Jet shapes

Apart from mass, other jet variables are used for QCD studies (e.g. tuning) and to identify jet type. ATLAS measured:

- Number of R=0.2 anti-kt subjets with pT > 10 GeV
- Les Houches angularity:

$$\lambda^{\kappa}_{\beta^{\mathrm{LHA}}} = \sum_{i \in J} z_i^{\kappa} \theta_i^{\beta^{\mathrm{LHA}}}$$

  where z is the momentum fraction and θ the angle wrt jet axis of the i[th] component, with (k = 1, β = 0.5)

- Energy Correlation ratios, C2 and D2

$$\mathrm{ECF1} = \sum_{i \in J} p_{\mathrm{T}_i},$$

$$\mathrm{ECF2}(\beta^{\mathrm{ECF}}) = \sum_{i<j \in J} p_{\mathrm{T}_i} p_{\mathrm{T}_j} \left(\Delta R_{ij}\right)^{\beta^{\mathrm{ECF}}},$$

$$\mathrm{ECF3}(\beta^{\mathrm{ECF}}) = \sum_{i<j<k \in J} p_{\mathrm{T}_i} p_{\mathrm{T}_j} p_{\mathrm{T}_k} \left(\Delta R_{ij} \Delta R_{ik} \Delta R_{jk}\right)^{\beta^{\mathrm{ECF}}},$$

$$e_2 = \frac{\mathrm{ECF2}}{(\mathrm{ECF1})^2}, \qquad C_2 = \frac{e_3}{(e_2)^2},$$

$$e_3 = \frac{\mathrm{ECF3}}{(\mathrm{ECF1})^3}. \qquad D_2 = \frac{e_3}{(e_2)^3}.$$

- N-subjettiness ratios $\tau_{21} = \frac{\tau_2}{\tau_1}$ and $\tau_{32} = \frac{\tau_3}{\tau_2}$ (used to distinguish W and top jets)

$$\tau_0(\beta^{\mathrm{NS}}) = \sum_{i \in J} p_{\mathrm{T}_i} R_0^{\beta^{\mathrm{NS}}},$$

$$\tau_1(\beta^{\mathrm{NS}}) = \frac{1}{\tau_0(\beta^{\mathrm{NS}})} \sum_{i \in J} p_{\mathrm{T}_i} \Delta R_{a_1,i}^{\beta^{\mathrm{NS}}},$$

$$\tau_2(\beta^{\mathrm{NS}}) = \frac{1}{\tau_0(\beta^{\mathrm{NS}})} \sum_{i \in J} p_{\mathrm{T}_i} \min(\Delta R_{a_1,i}^{\beta^{\mathrm{NS}}}, \Delta R_{a_2,i}^{\beta^{\mathrm{NS}}}),$$

$$\tau_3(\beta^{\mathrm{NS}}) = \frac{1}{\tau_0(\beta^{\mathrm{NS}})} \sum_{i \in J} p_{\mathrm{T}_i} \min(\Delta R_{a_1,i}^{\beta^{\mathrm{NS}}}, \Delta R_{a_2,i}^{\beta^{\mathrm{NS}}} \Delta R_{a_3,i}^{\beta^{\mathrm{NS}}}),$$

Tagging W and top

Containment of the decay products of W and top depends on particle pT; in a radius R = 1.0, Ws fully contained above 500 GeV, top above 1000 GeV

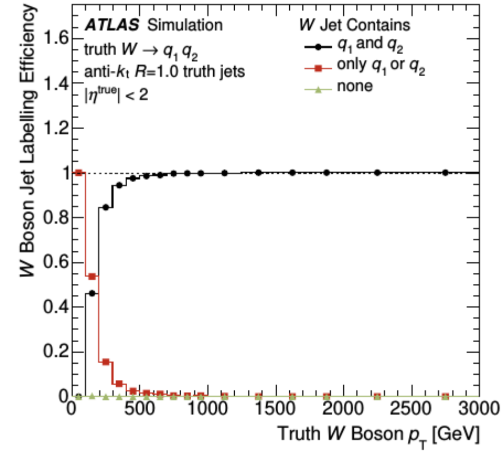

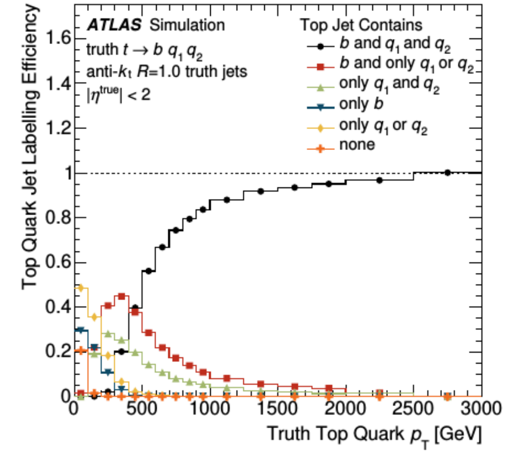

3 (5) approaches to tagging Ws (top):

- Mass + jet shape cut
- Boosted Decision Tree
- Deep Neural Network
  - Shower Deconstruction
  - HepTopTagger

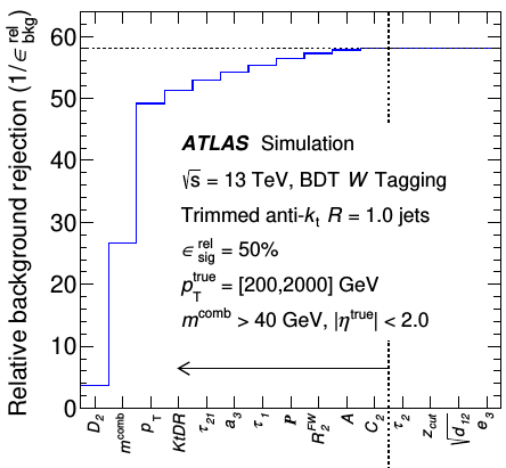

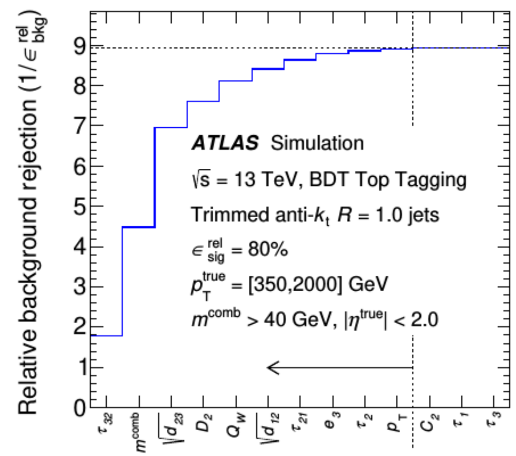

MC-based performance almost identical between BDT and DNN, much better than 2D cut (plot for top, similar for W)

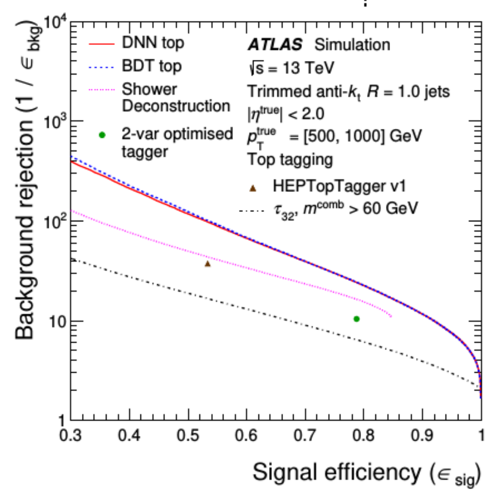

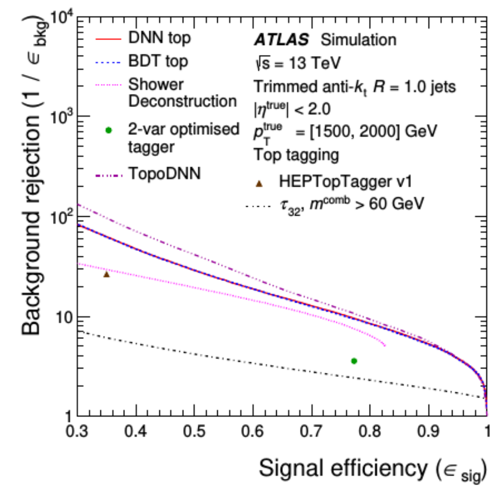

Eur. Phys. J. C 79 (2019) 375.

Measuring tagging performance on data

Semileptonic tt events ideal lab to have pure samples of jets from hadronic top and W decays

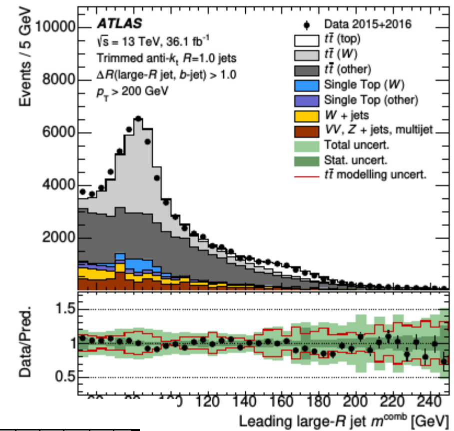

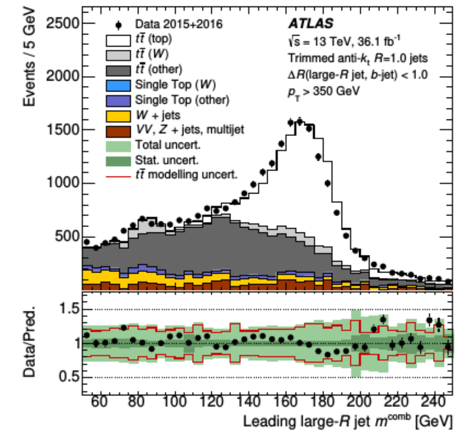

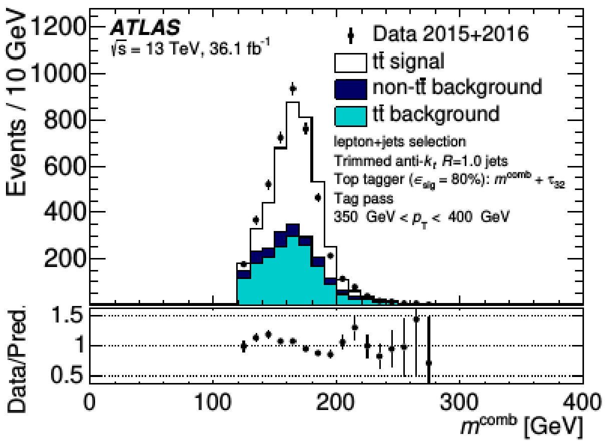

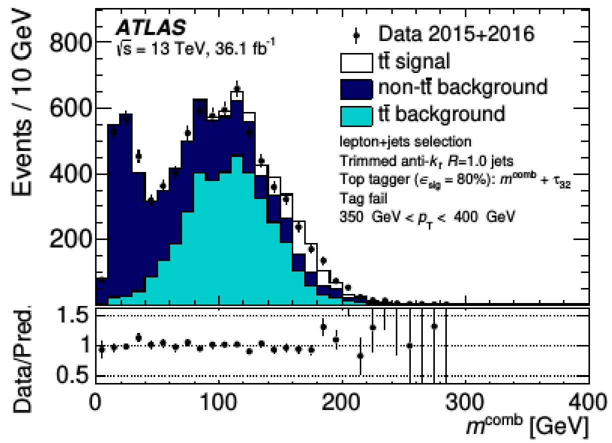

Efficiency derived from data from tagged and anti-tagged events

Background rejection extracted from multijet and gamma + jet events

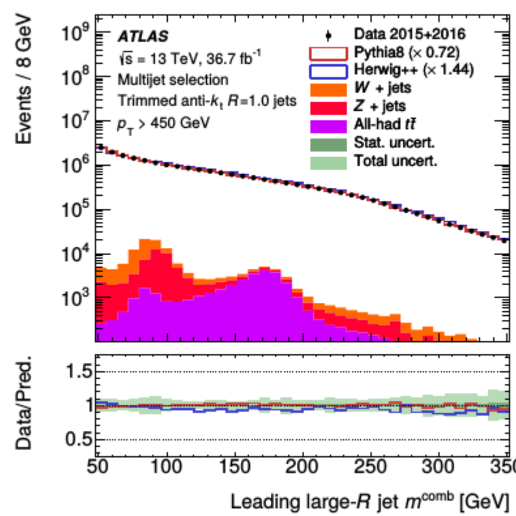

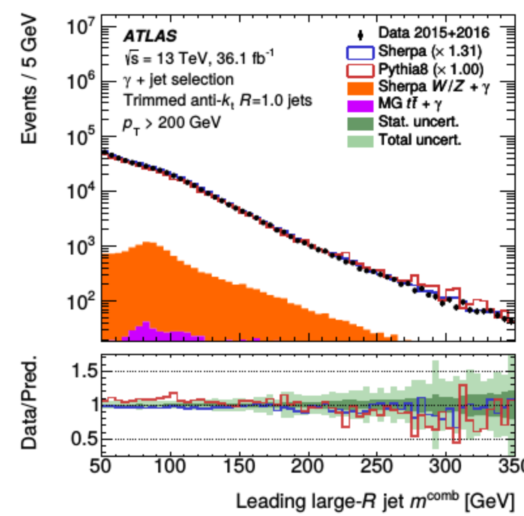

Tagging summary: data vs MC (W tag DNN example)

Efficiency

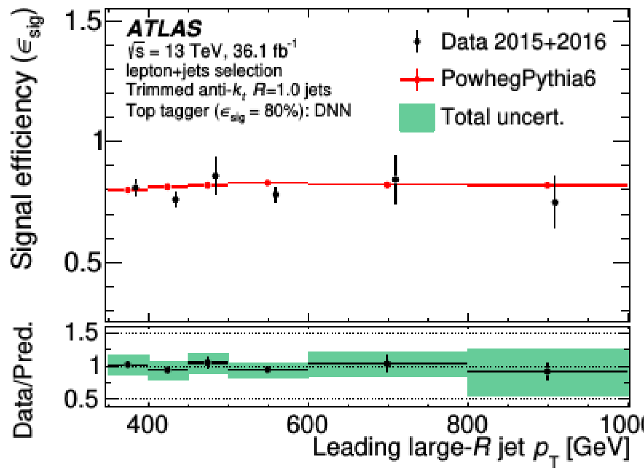

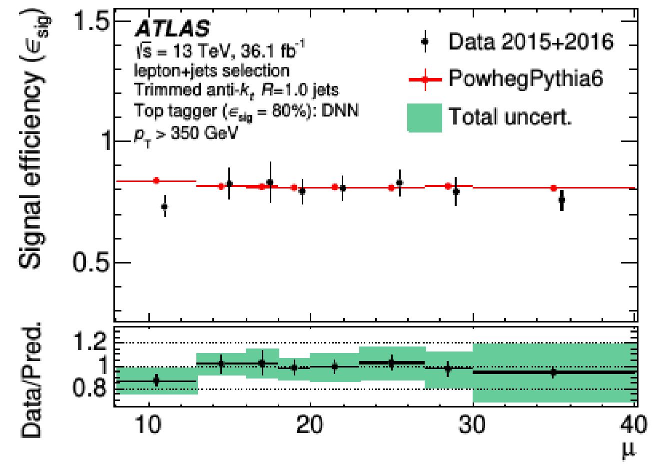

BG rejection

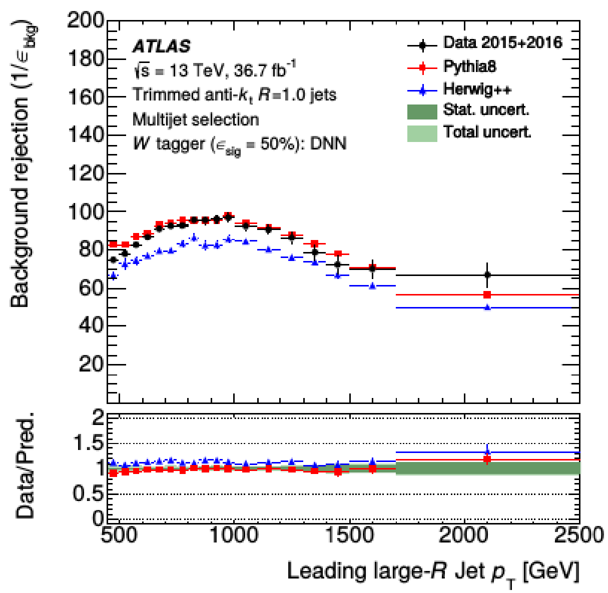

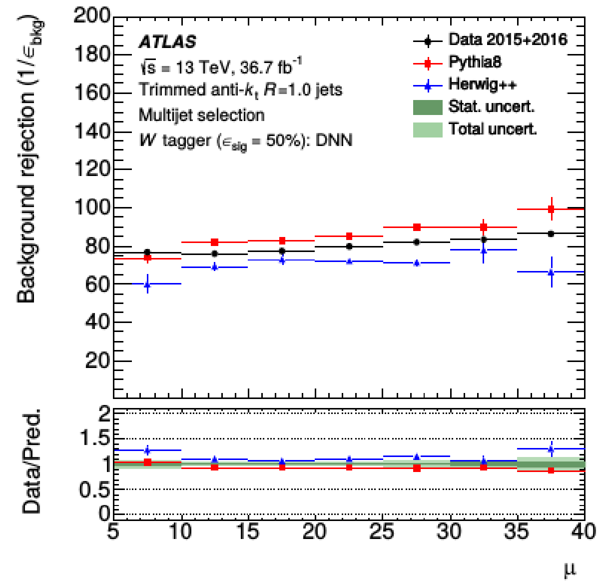

An improved groomer: SoftDrop

Trimmed jets are very stable wrt pileup, but the procedure is not analytically calculable- only possible to compare trimmed jets to MC (NNL precision)

The Soft-Drop algorithm clusters jet constituents with Cambridge-Aachen, and retraces the clustering history from the last branching. For each branch, it checks that

$$\frac{min(p_{T,j1}, p_{T,j2})}{(p_{T,j1} + p_{T,j2})} > z_{cut}(\frac{\Delta R_{j1,j2}}{R})^{\beta}$$

If it is satisfied, the algorithm stops.
If not, the soft branch j2 is removed, and the algorithm is applied recursively on j1.

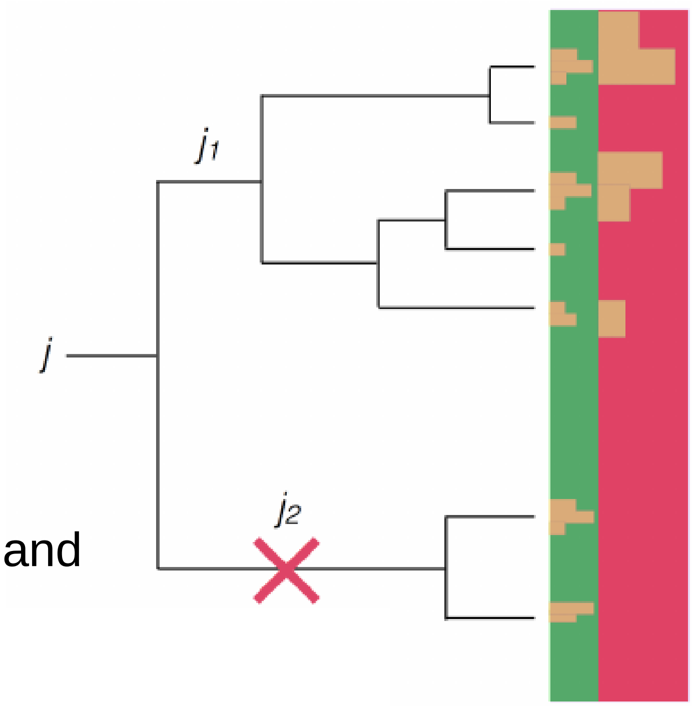

This procedure removes soft radiation, according to the scale z_{cut}, and large-angle emission, according to the parameter β (chosen)

In most ATLAS analyses, event selection is based on the calibrated trimmed jets; soft-drop can be applied instead of trimming to the jet ungroomed constituents to produce observables calculable at NLO + NLL

Jet mass in dijet events PhysRevLett.121.092001

- Event selection on ungroomed $R = 0.8$ jets:
  - $P_{T1} > 600$ GeV (to be on trigger plateau), $p_{T1} < 1.5 * p_{T2}$ (to select dijet events)
- Groom with SoftDrop ($z = 0.1$, $\beta = 0, 1, 2$)
- Groomed mass normalised to ungroomed p_T (collinear safe for $\beta = 0$) for more stability:

$$\rho = \log[(m^{\text{Soft Drop}} / p_T^{\text{Ungroomed}})^2]$$

- Normalised to data in the resummation region

  $-3.7 < \rho < -1.7$

Uncertainties

- Detector-level and particle-level quite different
  - Large off-diagonal terms in unfolding
- Differences between MC models
  - MC modeling dominant uncertainty

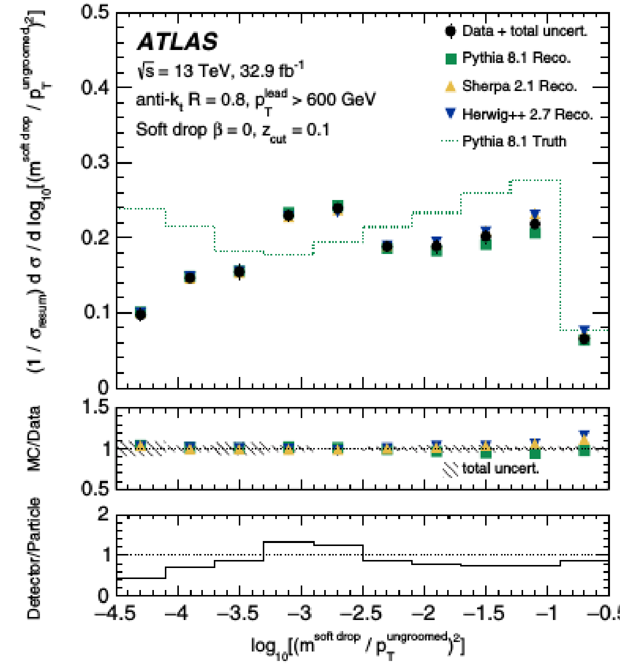

- Cluster uncertainties:
  - Energy scale large at small masses (low mult.)
  - Angular and energy smearing large at large masses

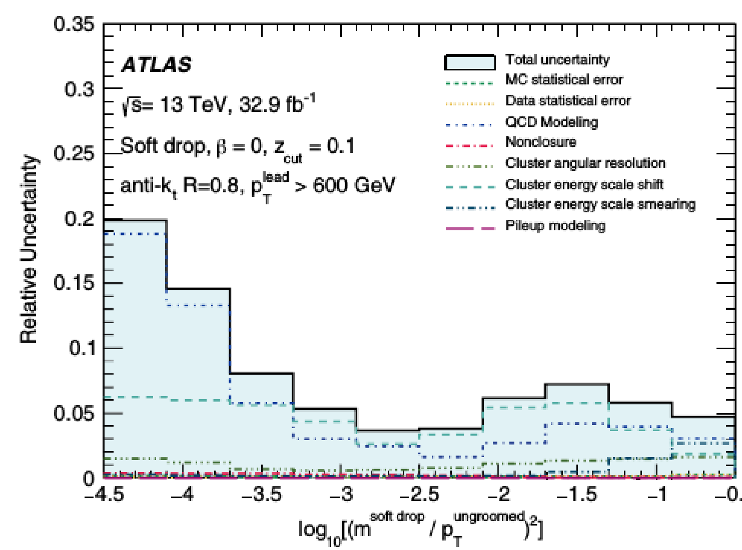

Results

Regions probed:

- Non-perturbative
- Resummation
- Fixed-order

Good agreement with MC (some discrepancies at low-mass)

Comparison with calculations requires NLO + NLL + NP to agree beyond resummation region

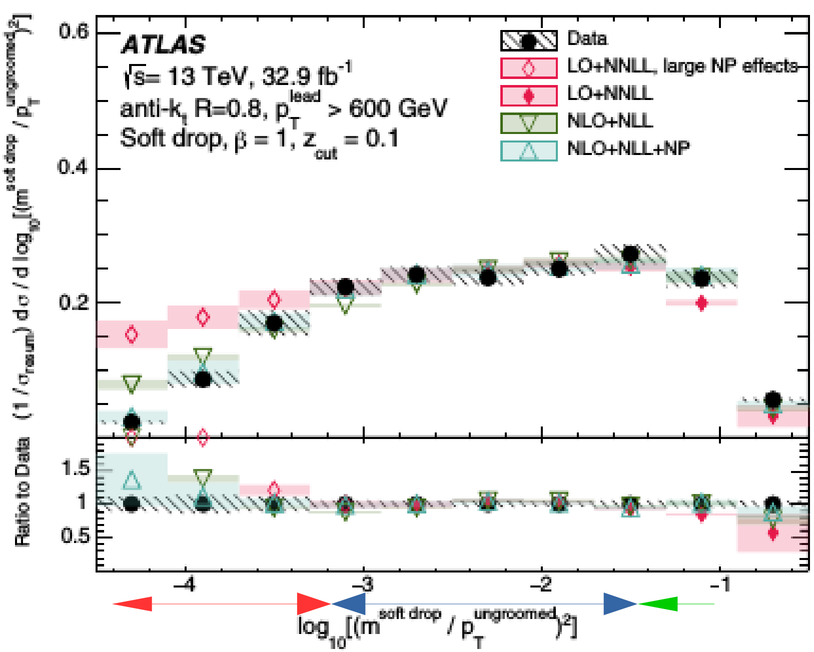

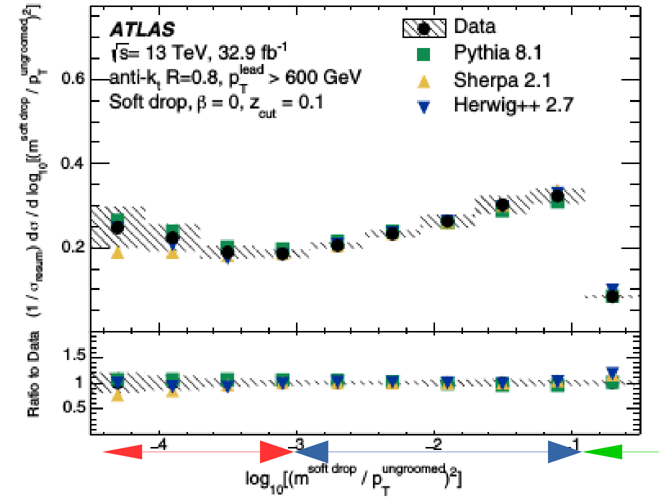

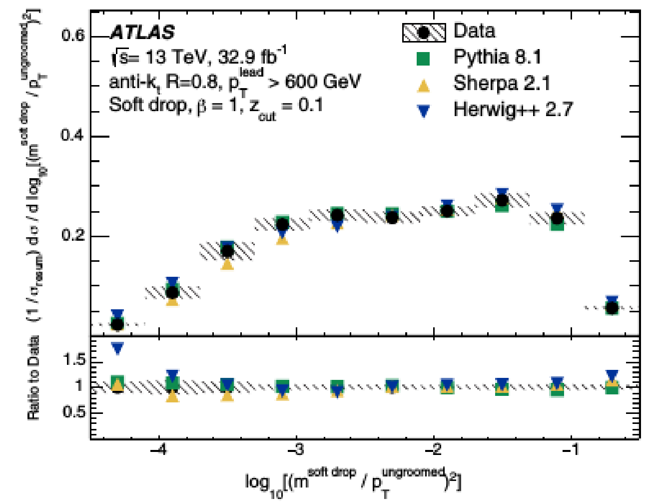

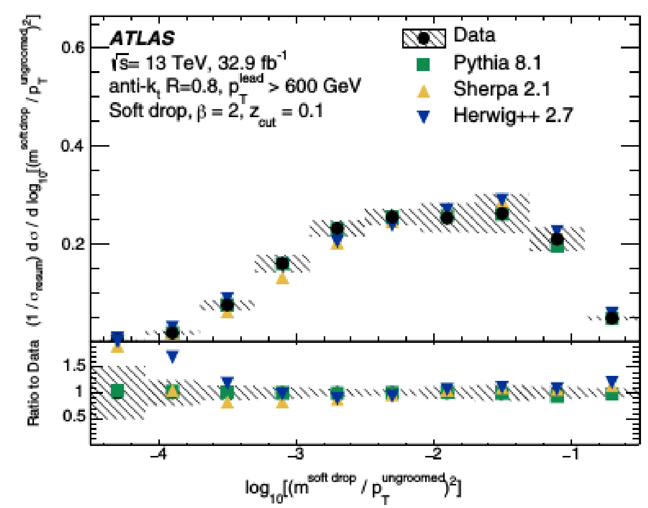

Jet-shape measurements for top, W and dijets: event selections

	Detector level	Particle level
Dijet selection:		
Two trimmed anti-k_t $R = 1.0$ jets	$p_T > 200$ GeV $\lvert\eta\rvert < 2.0$	$p_T > 200$ GeV $\lvert\eta\rvert < 2.0$
Leading-p_T trimmed anti-k_t $R = 1.0$ jet	$p_T > 450$ GeV	
Top and W selections:		
Exactly one muon	$p_T > 30$ GeV $\lvert\eta\rvert < 2.5$ $\lvert z_0 \sin(\theta)\rvert < 0.5$ mm and $\lvert d_0/\sigma(d_0)\rvert < 3$	$p_T > 30$ GeV $\lvert\eta\rvert < 2.5$
Anti-k_t $R = 0.4$ jets	$p_T > 25$ GeV $\lvert\eta\rvert < 4.4$ JVToutput > 0.5 (if $p_T < 60$ GeV)	$p_T > 25$ GeV $\lvert\eta\rvert < 4.4$
Overlap removal using small-radius jets	if $\Delta R(\mu, \text{jet}) < 0.04 + 10\ \text{GeV}/p_{T,\mu}$: Muon is removed, so the event is discarded	None
E_T^{miss}, m_T^W	$E_T^{miss} > 20$ GeV, $E_T^{miss} + m_T^W > 60$ GeV	
Leptonic top	At least one small-radius jet with $0.4 < \Delta R(\mu, \text{jet}) < 1.5$	
Top selection:		
Leading-p_T trimmed anti-k_t $R = 1.0$ jet	$p_T > 300$ GeV, mass > 140 GeV ΔR(large-radius jet, b-tagged jet) < 1 $\Delta\phi(\mu$, large-radius jet) > 2.3	
W selection:		
Leading-p_T trimmed anti-k_t $R = 1.0$ jet	$p_T > 300$ GeV, mass > 60 GeV and mass < 100 GeV $1 < \Delta R$(large-radius jet, b-tagged jet) < 1.8 $\Delta\phi(\mu$, large-radius jet) > 2.3	

Two separate event selections:

- Dijets
- Semi-leptonic tt
  - Top jets
  - W jets

Selection based on trimmed jets, jet shape measurement for both trimmed and soft-drop

ArXiv: 1903.02942

Detector-level distributions

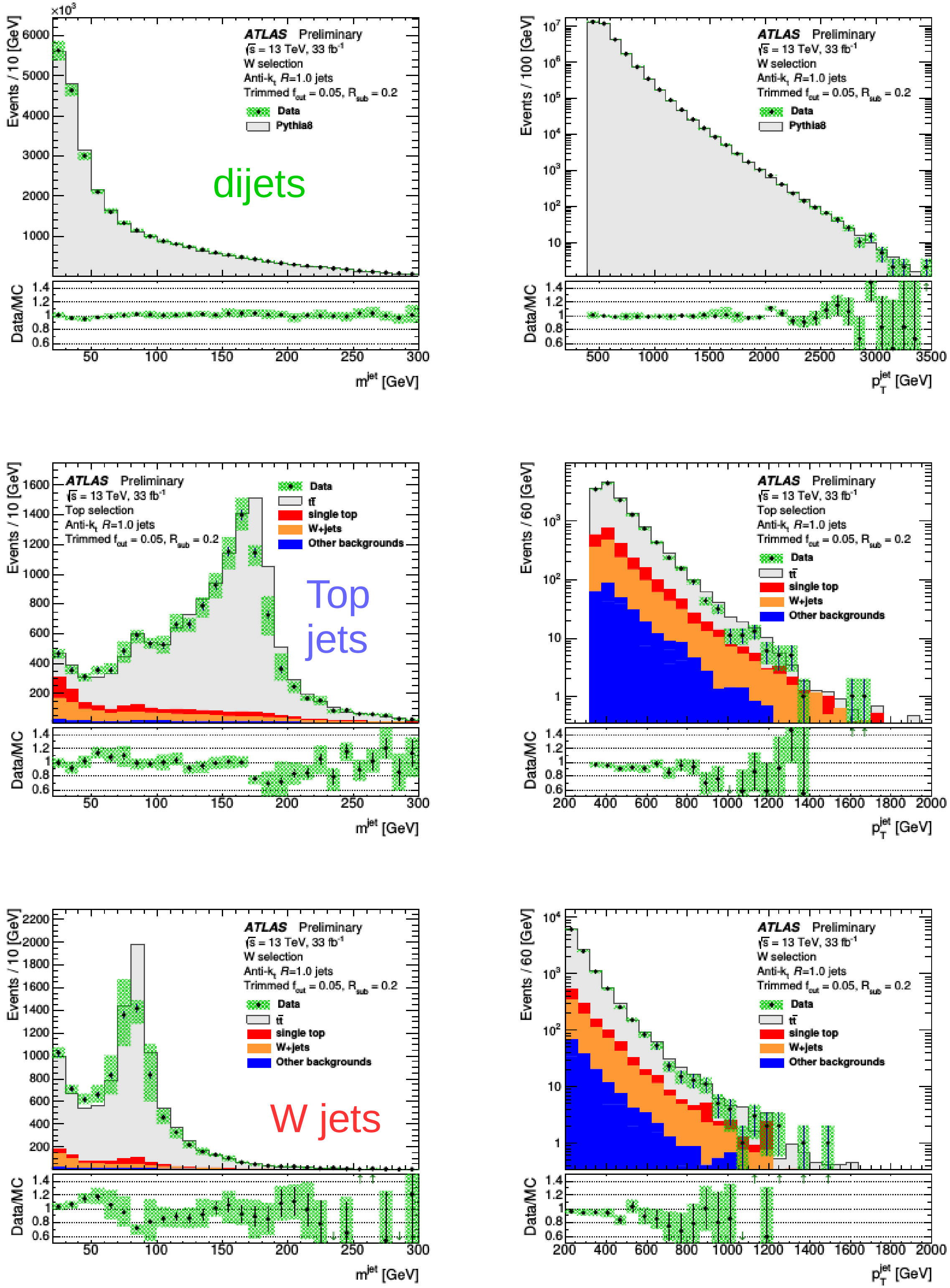

A Data-MC shift is observed in the detector-level mass, because no in-situ calibration is applied in this analysis.

The mass window for jet selection has been chosen to account for this effect.

Multiplicity

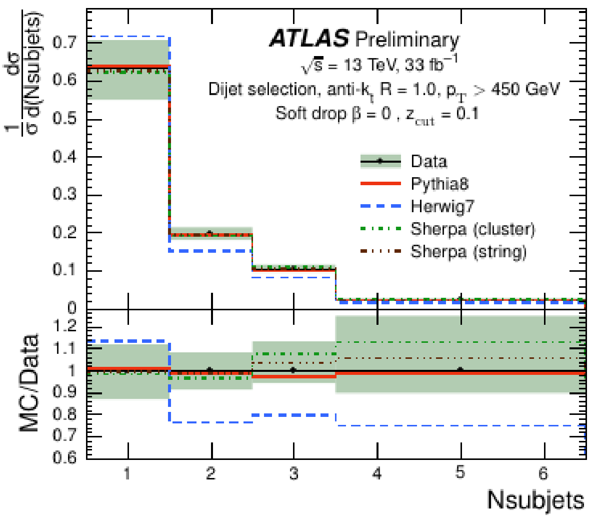

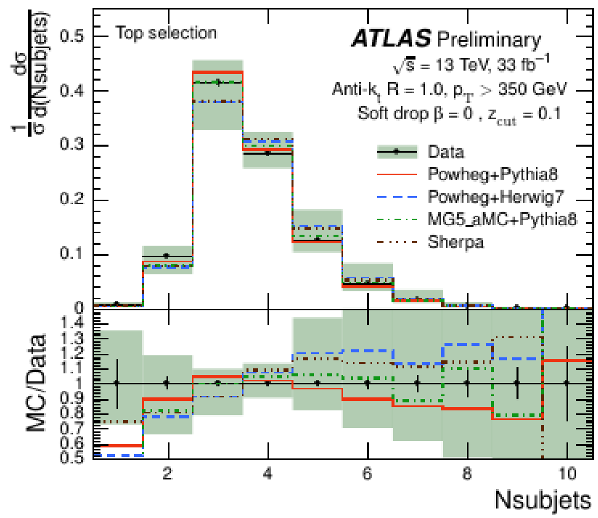

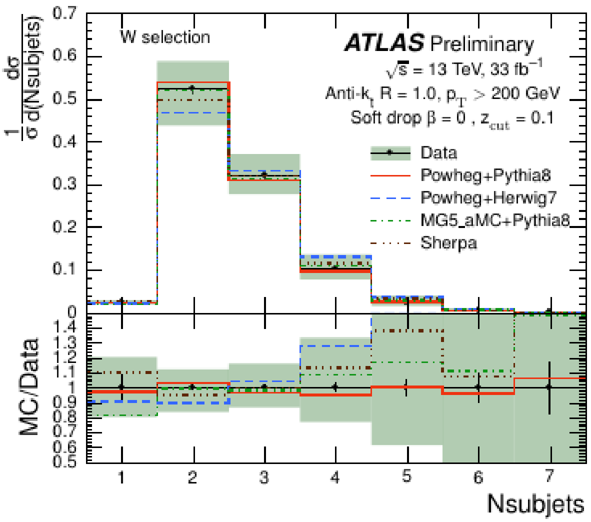

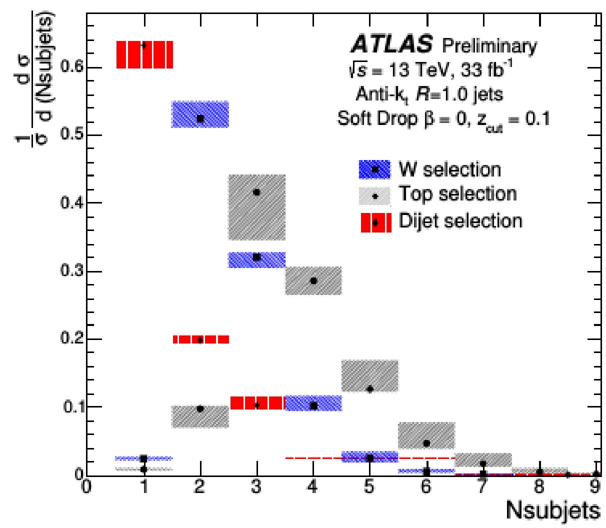

Largest uncertainties from calibrations: jet pT and mass calibration for selection, and clusters. Herwig 7 shows large disagreement for dijets

Angularity

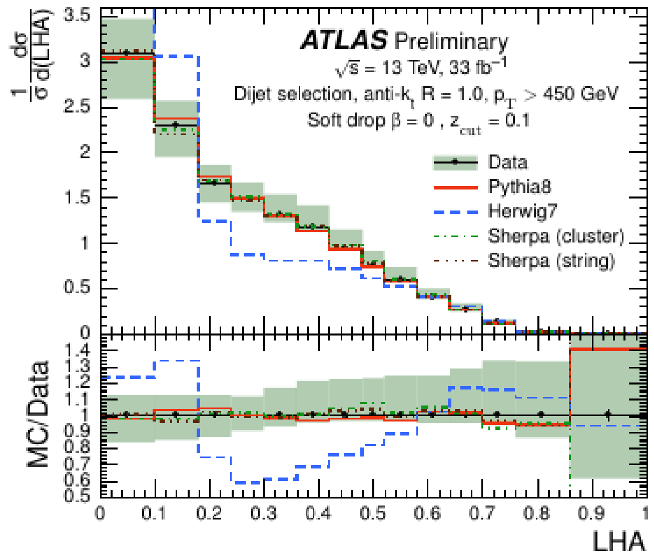

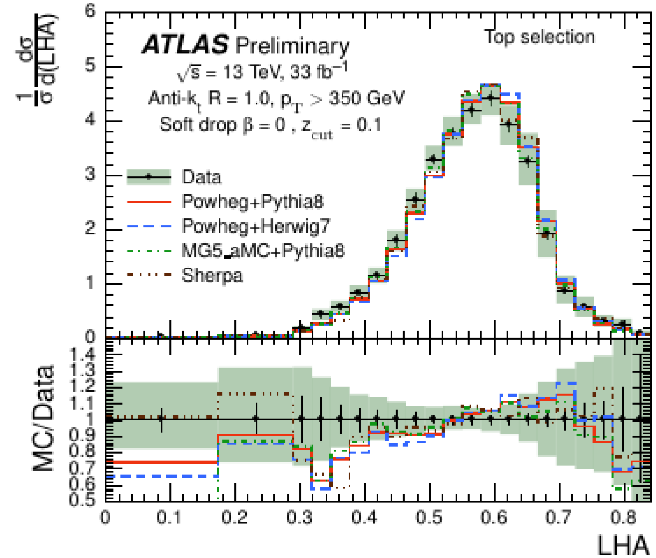

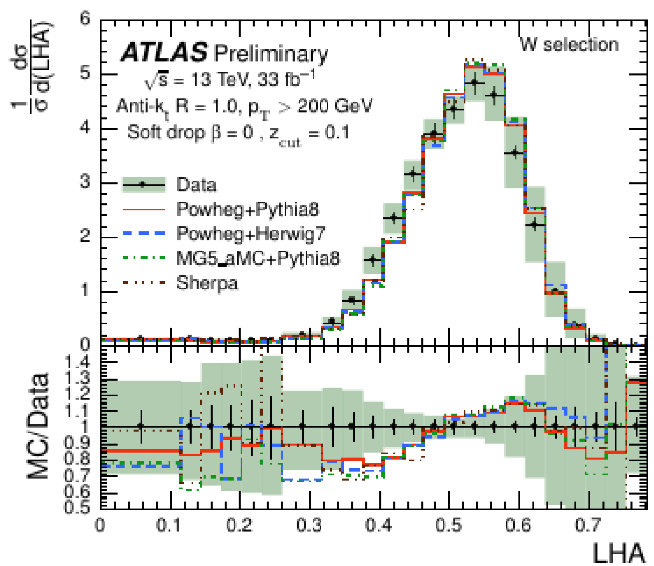

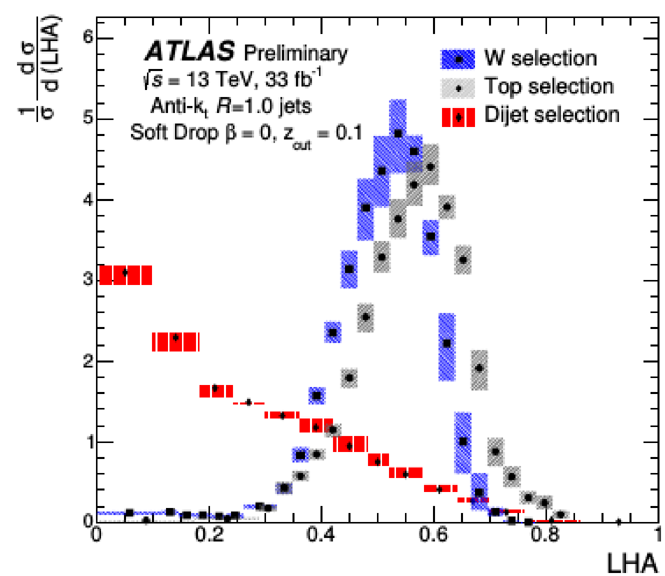

All models show tensions in W/top

D2

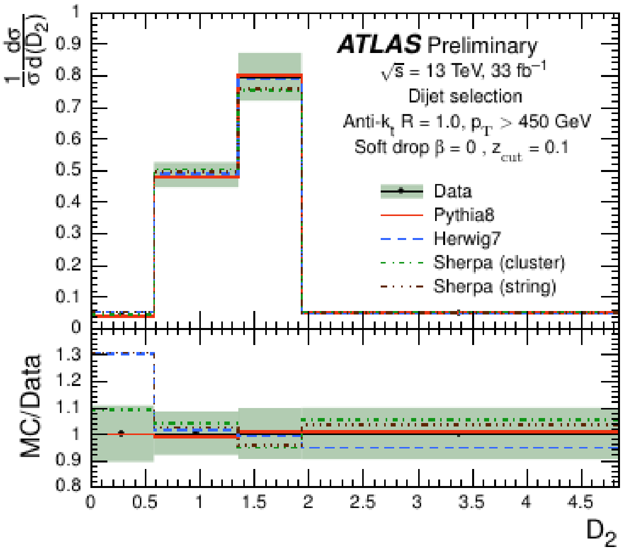

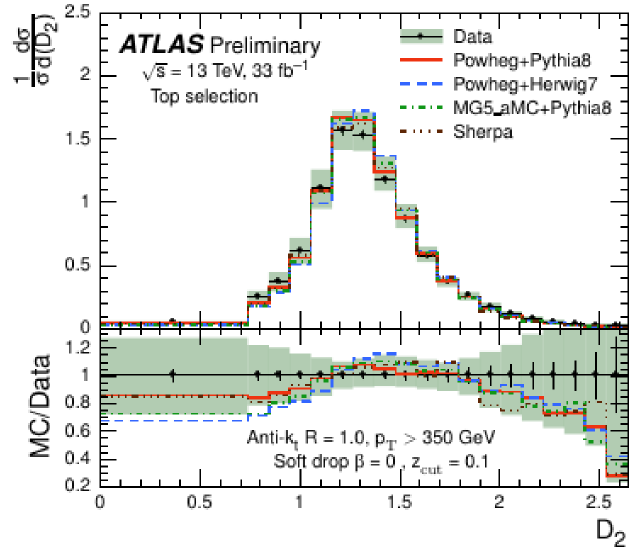

Widely used variable for W tagging

Significant shifts observed for all MC models in W events.

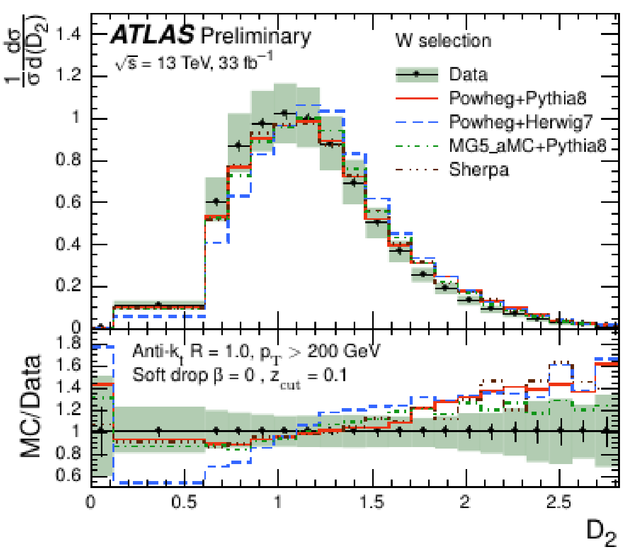

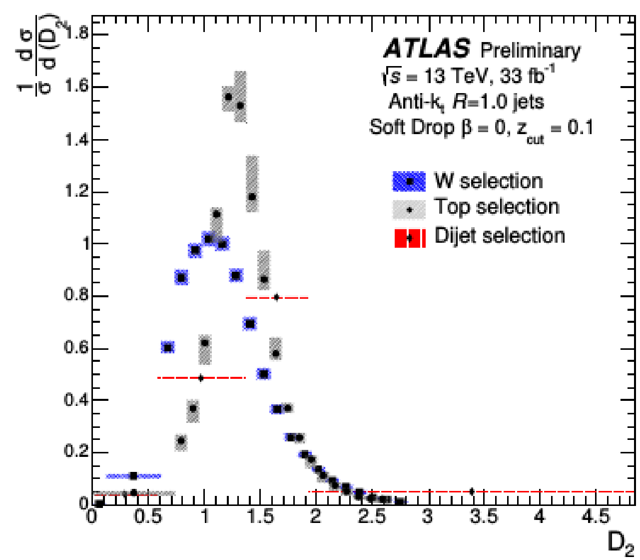

N-subjettiness τ_{21},τ_{32}

Used for W/top separation

Dijet events have less hard splitting, so are more sensitive to cluster split-merge uncertainties, that lead to very large errors

→ no dijet measurements for n-subjettiness

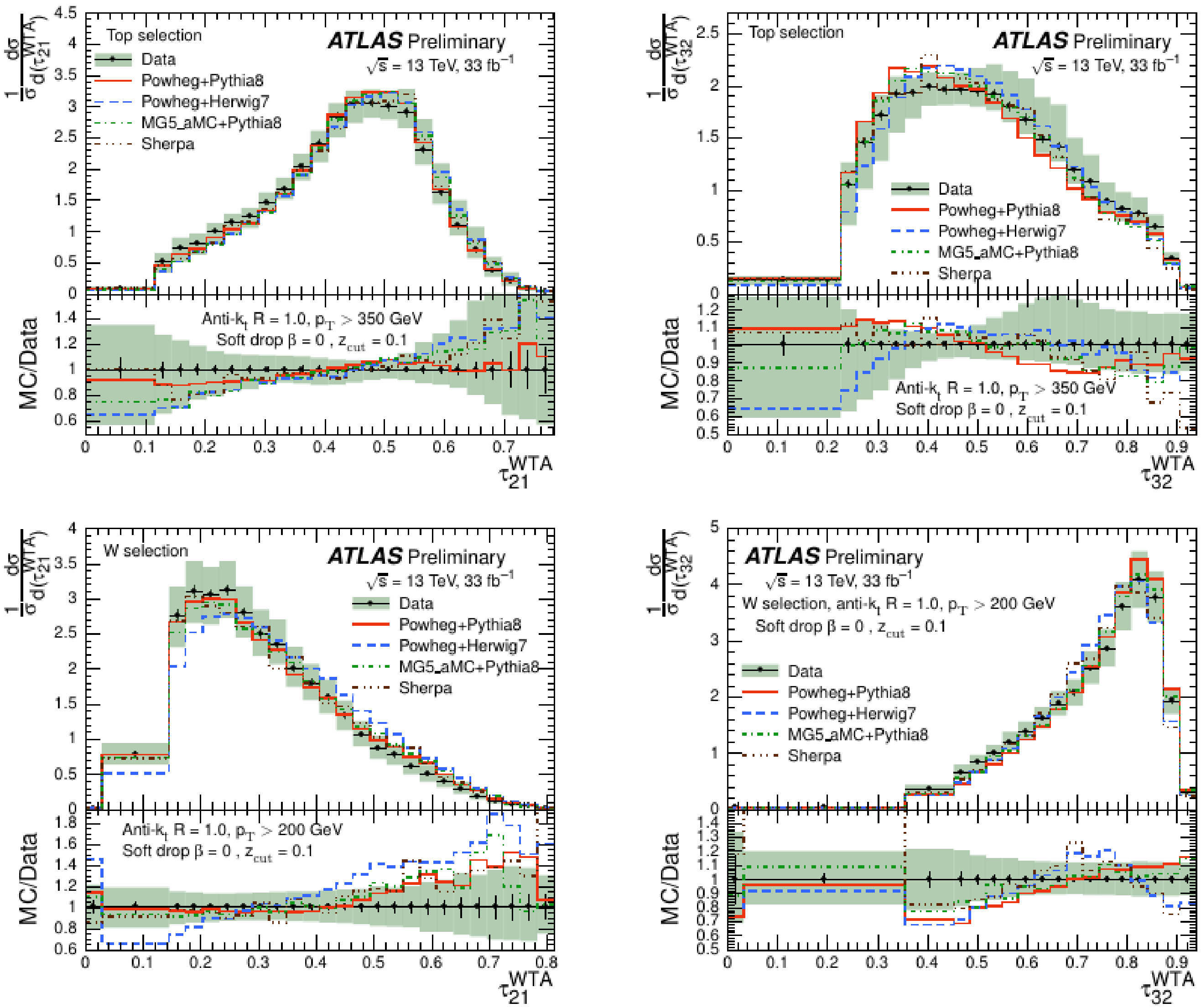

Conclusions

- Jet substructure is widely used in searches for heavy states decaying into boosted objects like top and W
- Several tagging methods used, mainly combining jet shape variables using multivariate techniques
- Its MC modelling is difficult, and measurements are needed to help improve it
- With careful control of uncertainties at jet and cluster level, precisions of O(10%) in the bulk of distributions and O(20%) in the tails are now possible, helping to discriminate models
- Additional performance work, and the possibility of higher-order calculations provided by SoftDrop will provide more stringent tests in the near future.